Highly Conductive, Flexible, Polyurethane-Based Adhesives for Flexible and Printed Electronics

*Zhuo Li, Rongwei Zhang, Kyoung-Sik Moon, Yan Liu, Kristen Hansen, Taoran Le, and C. P. Wong**

Flexible interconnects are one of the key elements in realizing next-generation flexible electronics. While wire bonding interconnection materials are being deployed and discussed widely, adhesives to support flip-chip and surface-mount interconnections are less commonly used and reported. A polyurethane (PU)-based electrically conductive adhesive (ECA) is developed to meet all the requirements of flexible interconnects, including an ultralow bulk resistivity of $\approx 1.0 \times 10^{-5}$ Ω cm that is maintained during bending, rolling, and compressing, good adhesion to various flexible substrates, and facile processing. The PU-ECA enables various interconnection techniques in flexible and printed electronics: it can serve as a die-attach material for flip-chip, as vertical interconnect access (VIA)-filling and polymer bump materials for 3D integration, and as a conductive paste for wearable radio-frequency devices.

1. Introduction

Modern consumer electronics are striving for increased functionality. Mechanical flexibility becomes an important trend for electronics because of the natural integration and increased functionality impossible within the confines of rigid, planar substrates. For example, flexible electronics enable applications where circuits are wrapped conformally around complex shapes or rolled up for storage, such as flexible displays,[1] flexible and conformal antennas,[2,3] thin-film transistors,[4,5] sensors arrays,[6] electronic solar-cell arrays,[7,8] and flexible energy-storage devices.[9,10] However, flexible electronics impose stringent requirements for interconnect materials.[11–14] In addition to the conventional functions of providing sufficient power, ground, and signal transmission, interconnects for flexible electronics are required to maintain excellent mechanical robustness and electrical interconnectivity during mechanical deformation.

While metal wires with elegantly designed structures[13,15–20] and ink-jet printed metal patterns[3,21–23] have been demonstrated to wire-bond chips to flexible substrates, there are considerably fewer reports on adhesive materials to support the flip-chip interconnects or surface-mount technology (SMT) for flexible electronics. Sn-based eutectic solders cannot be used in flexible electronics, because the high process temperature will damage the flexible, low-cost substrates such as paper and poly(ethylene terephthalate) (PET). Conventional epoxy-based electrically conductive adhesives (ECAs) suffer from the rigidity while silicone-based ECAs usually have limited conductivity (resistivity > 2.0×10^{-4} Ω cm).[24,25] Therefore, ECAs with high electrical conductivity, low process temperature, good mechanical compliance, and strong adhesion are needed to enable SMT and flip-chip interconnection on flexible and low-cost substrates in flexible electronics.

Here, we describe a novel approach to develop polyurethane (PU)-based flexible ECA (PU-ECA) that can meet all of the above requirements. By selecting the appropriate resin, the PU-ECA exhibits excellent electrical conductivity (resistivity ≈ 1.0×10^{-5} Ω cm) and the resistivity does not change when bending at a 2.64% flexural strain, rolling at a radius of 8 mm or pressing under 250 kPa. Additionally, the adhesion strength is much better than that of a commercial ECA (Ablethern 3188) and pure PU resin. The PU-ECA in this study demonstrates many other advantages, including a low curing temperature (150 °C), which enables printing and curing on low-cost flexible substrates; simple and cost-effective processing, by eliminating the use of any expensive silver nanoparticles[26,27] or additives[28,29] to achieve high electrical conductivity; and environmental-friendliness. These excellent material properties will be very promising for existing conductive adhesive interconnections and emerging flexible electronics.

2. Results and Discussion

2.1. Optimization of PU-ECA Formulation

The PU-ECA is prepared by a facile process. The PU resin used is methylethylketoxime (MEKO)-blocked hexamethylene

Z. Li, Dr. R. Zhang, Dr. K.-S. Moon, Y. Liu, K. Hansen, Prof. C. P. Wong
School of Materials Science and Engineering
Georgia Institute of Technology
771 Ferst Drive, Atlanta, GA, 30332, USA
E-mail: cp.wong@mse.gatech.edu
T. Le
School of Electrical and Computer Engineering
Georgia Institute of Technology
85 5th Street NW, Atlanta, GA, 30308, USA
Prof. C. P. Wong
Department of Electronic Engineering
The Chinese University of Hong Kong
Shatin NT, Hong Kong SAR, P.R.China

DOI: 10.1002/adfm.201202249

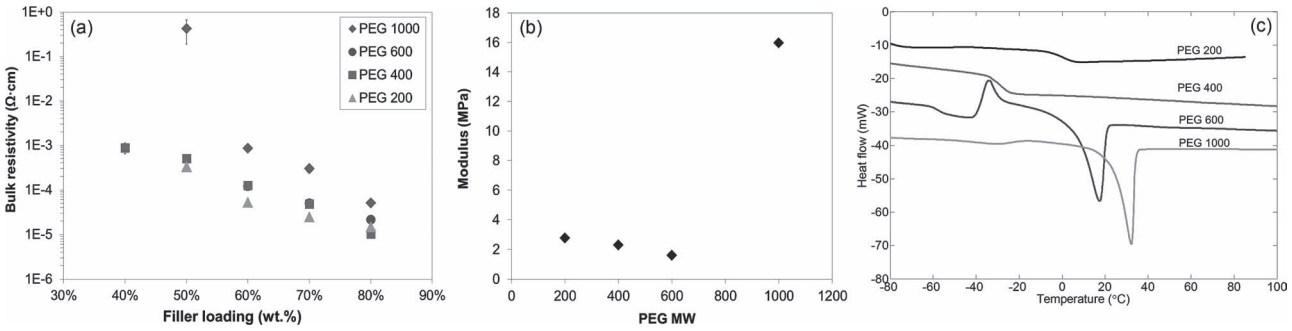

Figure 1. a) Bulk resistivity of PU ECAs as a function of silver loading for PU resin prepared with PEG of different molecular weights. b) Young's modulus of PU resin prepared with PEG of different molecular weights. c) DSC results of PU resin prepared with PEG of different molecular weights.

diisocyanate (HDI) cured by poly(ethylene glycol) (PEG). Two silver flakes with different sizes (0.8–2 μm and 1.9–5.5 μm, respectively) are used because such a bimodal size of fillers is reported to enhance the packing efficiency and thus decrease the viscosity of the paste.[27,30,31] The optimal chain length of PEG is found based on three aspects: the low bulk resistivity of the PU-ECA, low Young's modulus, and low glass-transition temperature (T_g) of the PU cured with PEG.

The bulk resistivity of PU-ECA prepared with PEG of different lengths is shown in **Figure 1**a. The resistivity increases with PEG chain length at the same filler loading, especially with a molecular weight up to 1000 g mol^{-1} (PEG 1000).

The Young's moduli decrease with the increase of PEG molecular weight from 200 to 600 g mol^{-1} (Figure 1b). PEG forms the soft segment of the PU resin and an increase of the soft segment usually leads to a lower Young's modulus. However, the Young's modulus shows a sudden increase when the molecular weight reaches 1000 g mol^{-1}. This is because the long PEG segments form crystalline structures, and the melting point of the crystallites for PEG with molecular weight of 1000 g mol^{-1} is around 37 °C (Figure 1c). At room temperature, the partially crystallized PU thus has a much higher modulus than other formulations with amorphous structures do.

The DSC results of cured PU with different PEG chain lengths are shown in Figure 1c. PEG with molecular weights of 200 g mol^{-1} (PEG 200) and 400 g mol^{-1} (PEG 400) does not form crystallites while PEG 400 has a lower T_g (–25 °C) than that of PEG 200 (6 °C). The lower T_g renders consistent mechanical properties in a larger temperature window. Therefore, PEG 400 is selected in an optimized formulation for PU-ECA.

2.2. Properties of PU-ECA

2.2.1. Bulk Resistivity and the Conduction Mechanism

The bulk resistivity as a function of curing temperature is shown in **Figure 2**a and the obtained resistivity can be as low as 1.0×10^{-5} Ω cm at 80 wt% silver loading when cured at 150 °C or above. The resistivity of PU-ECA (1.0×10^{-5} Ω cm) is one order of magnitude smaller than that of silver/polydimethylsiloxane (PDMS)[30] and silver/multiwalled nanotube (MWNT)/PDMS[28] composites, 2/3 less than that of silver-MWNT/nitrile butadiene rubber (NBR) composites,[29] and 1/2 that of epoxy ECA at the same process temperature.[27,31] It is also even lower than the reported resistivity of some printed silver-inks.[3,21] It is noted that, in prior studies, these high electrical conductivities are usually obtained by introducing silver nanoparticles[26,27] or silver-nanoparticle-decorated carbon nanotubes (CNTs),[28,29] because these nanoparticles can be sintered at relatively low temperatures (≈250 °C or below) to decrease the contact resistance.[26] However, the dispersion of metallic nanoparticles into the polymer matrix is quite challenging and the cost of nanoparticles is still high. In the case of PU-ECA, the ultrahigh electrical conductivity can be achieved simply by optimizing the formulation of the PU resin, instead of the use of expensive nanoparticles or complex preparation methods. Two possible factors contribute to the high conductivity of PU-ECA. The first factor is the significant shrinkage during curing of PU-ECA, which leads to an increased volume percentage of silver after curing. As shown in the thermal mechanical analysis (TMA) result (Figure 2b), the PU-ECA experiences significant volume shrinkage from 35 °C to 110 °C. Volume shrinkage during curing was also observed for epoxy-based ECA in previous reports while silicone-based ECA does not show obvious shrinkage (Supporting Information, Figure S1). According to previous studies,[32,33] such shrinkage can generate a compressive force to draw the silver flakes together and decrease the bulk resistivity. Here, the shrinkage of the PU matrix reduces the bulk resistivity of the PU-ECA from the upper limit of the measurement at 20 °C to as low as 10 Ω at 110 °C. After reaching 110 °C, thermal expansion exceeds the curing shrinkage while the resistance continues to drop at around 140 °C, indicating that factors other than the matrix shrinkage contribute to the improved conductivity at temperatures over 110 °C. The second possible factor is that the hydroxyl groups in the polyether chains can reduce the silver salts on the surface of silver flakes in situ to produce silver nanoparticles, which can be sintered during the curing of PU-ECA to form metallic bridges between neighboring flakes. As demonstrated by the Raman spectra (Supporting Information, Figure S2), the commercial silver flakes in use are coated with a thin layer of silver salts of fatty acids. This insulating layer helps to improve the processability but dramatically increases the contact resistance between the silver fillers inside the ECAs.[34–36] Polymers with hydroxyl groups such as PEG[37] and poly(vinyl alcohol)[38] have been extensively reported to reduce silver salts to silver

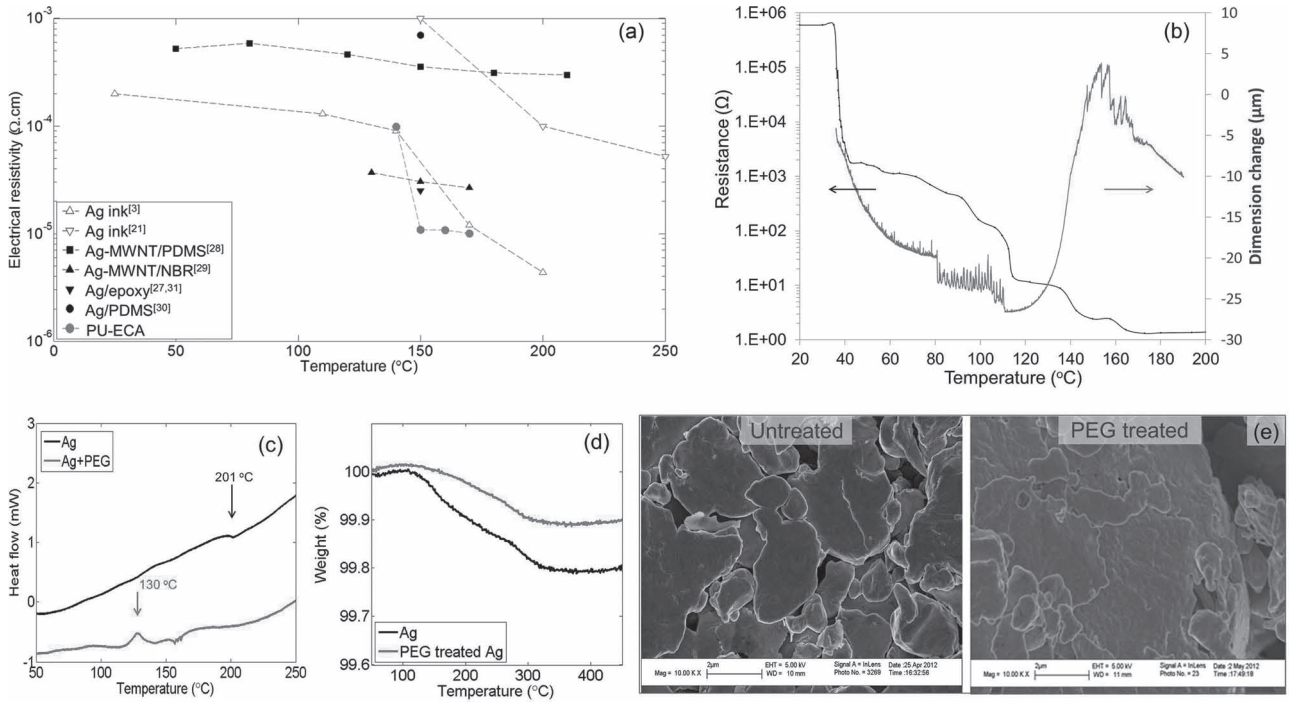

Figure 2. a) The bulk resistivity of PU-ECA cured at different temperatures as compared with other interconnect materials for flexible electronics. b) The bulk resistance and dimension change of PU-based ECA as a function of temperature. c) DSC results of silver flakes and silver flakes with PEG. d) The weight loss of untreated and PEG-treated silver flakes. e) SEM images of untreated and PEG-treated silver flakes.

nanoparticles effectively at mild conditions. PEG, used as a curing agent in this study, can also serve as a reducing agent to reduce silver carboxylate and generate silver nanoparticles during curing at 150 °C. Indeed, the DSC results (Figure 2c) of pure silver flakes show a small peak at 201 °C, corresponding to the thermal decomposition of the silver carboxylate.[31] When adding PEG to silver, the peak at at 201 °C in the DSC curve disappears; instead, an exothermic peak is observed at 130 °C, indicating the reduction reaction of silver carboxylate by PEG. In the thermogravimetric analysis (TGA) tests (Figure 2d), the untreated silver flakes show a weight loss of 0.20% when heated to 450 °C in a dynamic run due to the decomposition of surfactants on the silver flakes while the PEG-treated silver flakes show a significantly smaller weight loss of 0.10%, implying partial removal of surfactants by PEG. The formation of nanoparticles by a reduction reaction is confirmed by scanning electronic microscopy (SEM). The untreated flakes show smooth surfaces, while, after heating at 150 °C with PEG for 30 min, the silver flakes clearly show some roughness owing to the growth of silver nano-/sub-micrometer-sized particles on their surfaces and edges (Figure 2e). Moreover, these grown sub-micrometer-/nanosized particles on the silver-flake surfaces are sintered, forming necking between the silver flakes. This necking metallically bridges neighboring flakes and thus significantly reduces the contact resistance between the silver flakes, corresponding to the resistance drop at 140 °C in Figure 2b. While the reduction of the silver carboxylate on the silver flakes by PEG acts in a similar way to the introduction of silver nanoparticles or silver nanoparticle-decorated CNTs, the silver carboxylate reduction process is more cost effective and efficient to improve the electrical conductivity.

2.2.2. Conductivity Under Mechanical Deformation

In addition to a high electrical conductivity in the static state, ECAs for flexible electronics need to maintain their conductivity under mechanical deformation. The storage modulus of a PU-ECA film at 25 °C is 1098 MPa, as measured using a dynamic mechanical analyzer (DMA), indicating a flexible structure. **Figure 3** shows the electrical resistivity change of PU-ECA films under various forms of mechanical deformation. First, the bending deformation of a free-standing PU-ECA film is made using a three-point bending fixture. The resistance change is less than 10% when bending at a flexural strain up to 2.64%. Moreover, the resistance stays constant even after 1000 cycles of bending. The same sample was also tested by rolling at different radii in a setup similar to that in a previous report.[29] The resistance does not change significantly when the radius is larger than 7 mm, though the resistivity does increase to 3.3×10^{-5}, 4.2×10^{-5}, and 6.8×10^{-5} Ω cm when rolling at 7.5, 5, and 3.5 mm respectively. The rough surfaces of the silver flakes and the necking between neighboring flakes from the PEG treatment (Figure 2e) help to maintain the contact between the fillers, and thus the resistivity, during moderate deformation. When the deformation increases to a certain level, the resistivity increases due to the loss of contact. The increased resistivity in

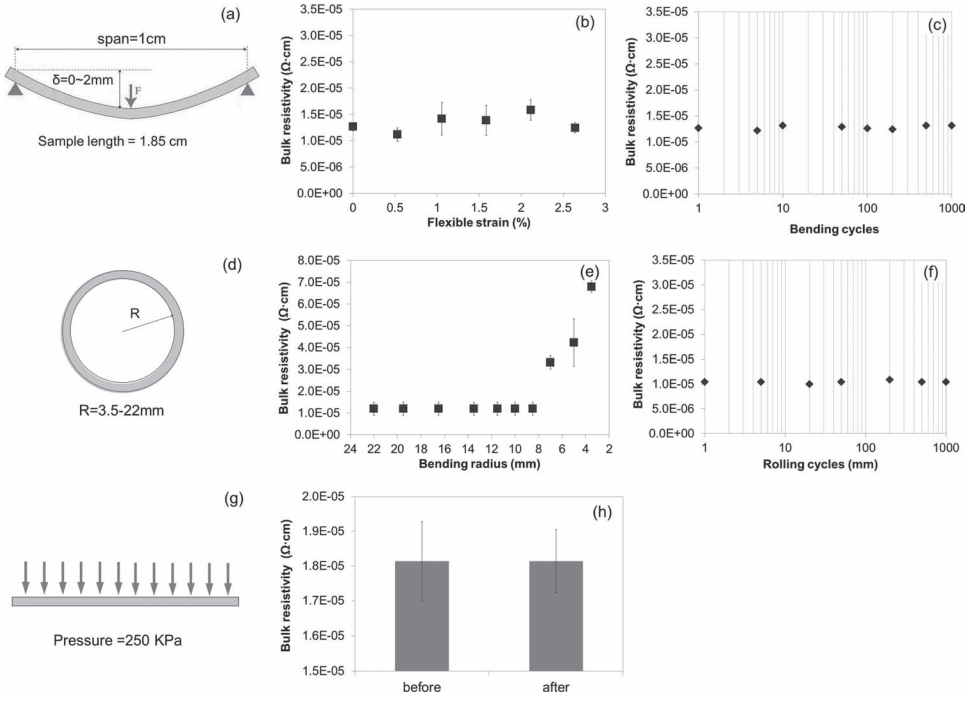

Figure 3. a) A schematic illustration of the three-point-bending test of the PU-ECA film. b) The electrical resistivity as a functional of flexural strain. c) The electrical resistivity as a function of bending cycle at a flexural strain of 2.64%. d) A schematic illustration of the rolling test of the PU-ECA film. e) The electrical resistivity as a functional of rolling radius. f) The electrical resistivity as a function of rolling cycle at a radius of 8 mm. g) A schematic illustration of the high-pressure test of the PU-ECA film. h) The electrical resistivity before and after high-pressure test.

the rolling test, however, is still lower than that of most silver-based composites reported.[21,28] A further cycling test shows that the resistivity is invariant after rolling at 8 mm for 1000 times. The normal pressure test on the PU-ECA film up to 250 kPa exhibits no change in resistivity. It should be noted that the thickness of the PU-ECA film tested here is around 360 μm, which is much larger than some previously reported bendable conductive materials (60 μm[29] and 20 μm[3]). In addition, the PU-ECA samples tested here are free-standing films while the samples tested by Sekitani et al.[3] and Ma et al.[29] are printed on a flexible substrate. Since the bending stiffness of a thin sheet is proportional to the cube of its thickness,[39] the PU-ECA could have the potential of exhibiting even better flexibility and electrical properties under deformation than the results shown in Figure 3, if the thickness of the samples is decreased.

2.2.3. Adhesion Strength

The adhesion of PU-ECA to photo-paper, PET, and polyimide (PI) substrates was measured by a standard tape test. No noticeable ECA materials were removed by the tape, indicating good adhesion of PU-ECA to these flexible substrates (**Figure 4**a). Moreover, a lap shear test was performed on two Cu strips bonded with PU of different silver loadings (Figure 4b). Compared with pure PU, the adhesion strength increases from 0.12 kg mm^{-2} to 0.14 kg mm^{-2} when the silver loading increases to 60 and 70 wt% loading. This increase may result from the increased modulus that helps with the interfacial strength. When the loading further increased to 80 wt%, the adhesion decreased to 0.125 kg mm^{-2} due to reduced flowability of the ECAs which causes incomplete asperity filling on bonding surfaces and a loss of contact area by inorganic fillers (Figure 4c). However, this value is still higher than either that of the pure PU resin or the commercial PU-based ECA (0.07 kg mm^{-2}, labeled 3188).

2.3. Demonstration of PU-ECA in Flexible Electronics

The PU-ECA in this study meets the requirements of interconnect materials in flexible electronics, such as high electrical conductivity, low process temperature, good mechanical compliance, and strong adhesion, which enables PU-ECA to be applied in a variety of flexible electronics.

2.3.1. PU-ECA as Interconnection Materials

PU-ECA can be used as die-attach materials for flexible electronics. Light-emitting-diode (LED) chips were attached to a PU-ECA pattern on a photo-paper substrate. The brightness of these LED chips was invariant for the flat (**Figure 5**a), and rolling state (Figure 5b,c, radii = 18.5 and 15 mm, respectively), indicating the excellent adhesion and power transmission of the PU-ECA.

Furthermore, the PU-ECA can increase the circuit integration density by providing multiple-layer structures. As shown in **Figure 6**a, a three-layer structure is built by drilling a vertical interconnect access (VIA) through the substrate and using

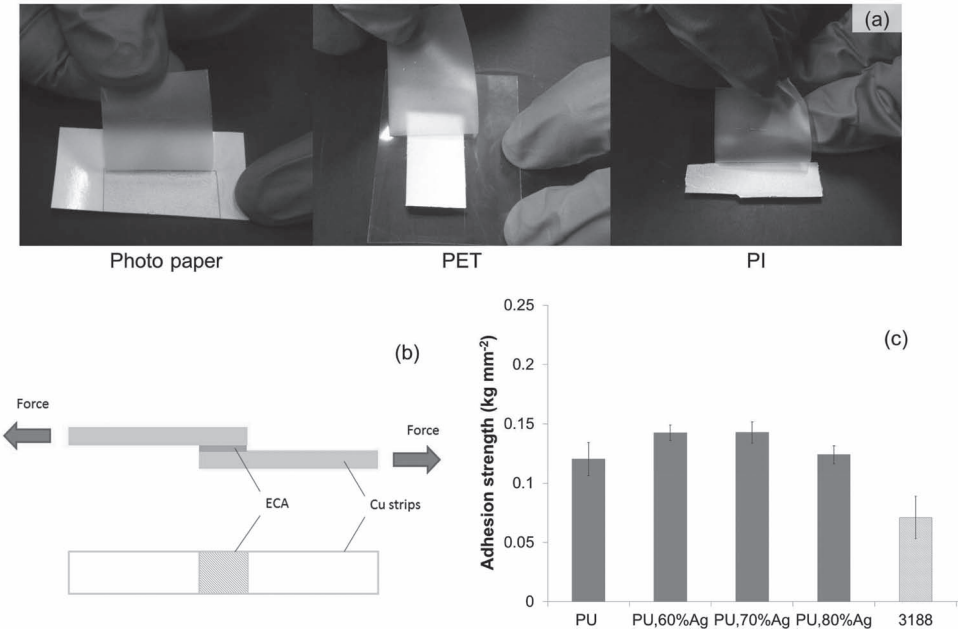

Figure 4. a) The adhesion of PU-ECA to different flexible substrates is investigated using scotch tape. b) Schematic illustration of the lap-shear test. c) Lap-shear-test results of PU-ECA with different silver loadings and Ablethern 3188 as a benchmark material.

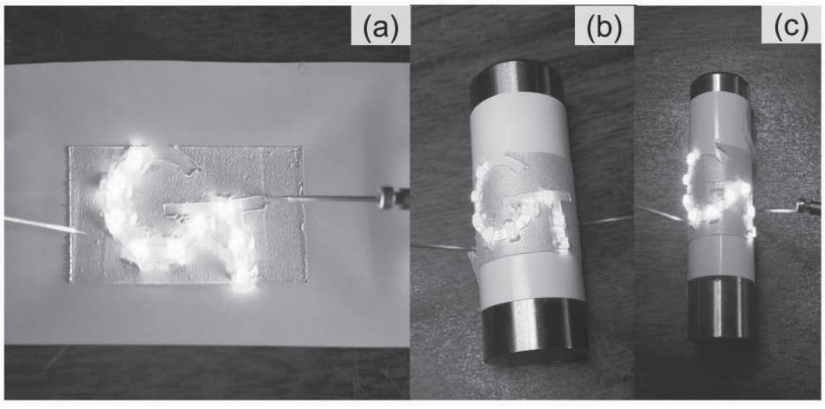

Figure 5. a) LED chips are attached to photo-paper substrate by PU-ECA. The brightness of the LED chips does not change when rolling at radius of 18.5 mm (b) and 15 mm (c).

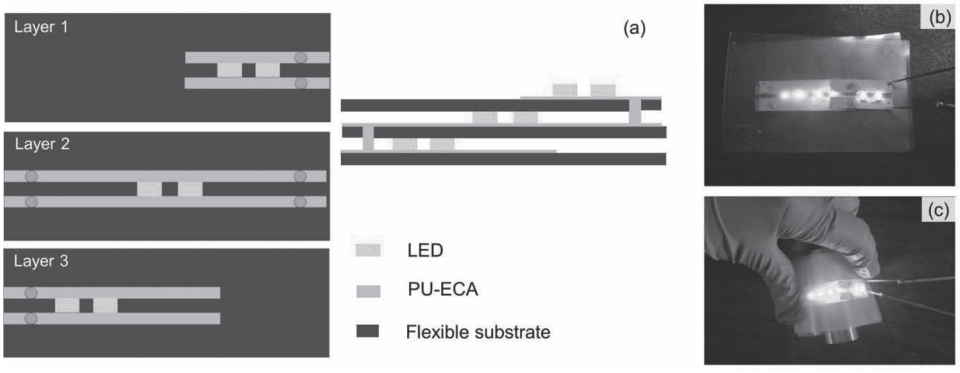

Figure 6. a,b) Configuration (a) and photo (b) of a three-layer structure built by drilling VIAs through each layer and using PU-ECA as *Z*-direction interconnects. Six LED chips are powered with two in each layer. c) The brightness does not change when the three-layer package is bent.

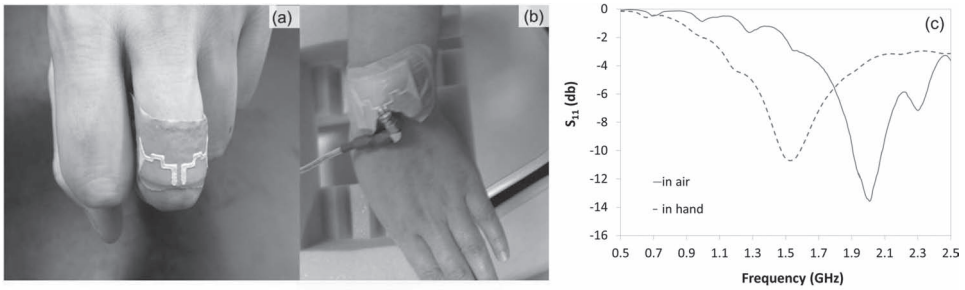

Figure 7. a) Flexible antenna made of PU ECA can be printed on bandage and wrapped around a finger. b) Testing an antenna on a wrist with a vector network analyzer (VNA). c) The S_{11} parameter of the antenna in the frequency range of 0.5 to 2.5 GHz.

PU-ECA as polymer bumps and VIA-filling materials. Each layer powers two LED chips. With the 3D structure, six LEDs in all three layers can be illuminated to provide more-intense light per unit area (Figure 6b). Additionally, this package can withstand a large deformation while maintaining its electrical functionality (Figure 6c).

2.3.2. Wearable Antennas

The flexible PU-ECA may also be used as flexible RF-devices. A flexible antenna is fabricated by stencil printing of PU-ECA on various substrates such as photo paper and bandage. As shown in **Figure 7**, PU-ECA printed on bandage can be bent and twisted without damaging the antenna pattern. From the simulation, within the range from 500 MHz to 5 GHz, the resonant frequency of the antenna is around 1.9 GHz. The resonant frequency of a free-standing antenna was measured to be 2.01 GHz, while, when the antenna is wrapped around a human wrist, the resonant frequency shifts to 1.53 GHz. The shift in resonant frequency may result from the influence of the electromagnetic properties of the human body as well as the physical deformation. In both cases, the S_{11} parameter is below 10 db, indicating the good performance of the printed flexible antenna.

3. Conclusions

In summary, the PU-ECA in this study offers a high electrical conductivity achieved by the polymer shrinkage and in situ formation of silver nanoparticles. The electrical resistivity reaches 1.0×10^{-5} Ω cm and remains stable when bending at 2.64% flexural strain, rolling at a radius of 8 mm or pressing under 250 kPa. It also has good adhesion to various flexible substrates and Cu surfaces. The combination of these properties will make PU-ECA a very promising interconnect material for flexible and printed electronics.

4. Experimental Section

Synthesis of PU-ECA: PEG (Sigma–Aldrich) was put into a vacuum pump for 6 h before mixing with HDI, (Bayer AG) and various amounts of silver flakes (Ferro Corp.). The two sizes of flakes were added with a ratio of 1:1. The mixture was homogenized for 5 min. Then, the paste was kept in a vacuum oven for 12 h to evaporate the solvents from the HDI prepolymer before curing.

The PEG chain length was optimized for a low modulus, high electrical conductivity and low glass-transition temperature. The Young's modulus was measured by tensile testing with an extension rate of 50 mm min^{-1} (Instron Microtester 5548). The glass-transition temperature and crystallization temperature were measured by DSC (TA Instrument Q2000). The bulk resistivity measurement is detailed in the following characterization section.

Characterization: To measure the electrical resistivity, the paste was cast in a polytetrafluoroethylene (Teflon) mold (22 mm × 7 mm × 0.5 mm). After curing at 150 °C for 1 h, the bulk resistance of the film was measured by the four-wire method with a Keithley 2000 multimeter. The thickness was measured using a profilometer (Heidenhain ND 281, Germany). The bulk resistivity ρ was then calculated by:

$$\rho = R\frac{wt}{l} \quad (1)$$

where l, w, and t are the length, width, and thickness of the film, respectively.

The Raman spectra of silver flakes were obtained using a LabRAM ARAMIS Raman confocal microscope (HORIBA Jobin–Yvon) equipped with a 532 nm diode-pumped solid-state (DPSS) laser. Si wafer was used as a substrate.

The dimensional change of the PU-ECA paste during thermal cure was measured using a TMA instrument with macroexpansion mode (TA instruments, Q400).[33] A small amount of the paste was sandwiched between two microscope cover glasses. The sample was cured in the TMA instrument and dimensional changes during curing were recorded. The static force of the probe was kept at 0.02 N to ensure that the adhesive paste was not squeezed out during heating. The heating rate was 5 °C min^{-1}.

Decomposition of the lubricants on the surface of silver flakes with and without PEG was studied by a modulated DSC (TA Instruments, Q2000). The heating rate was 1 °C min^{-1}.

PEG-treated silver flakes were prepared by immersing silver flakes in PEG at 150 °C for 30 min. The silver flakes lost their luster after being treated. Then PEG and surfactant reduction products were removed by adding acetone and centrifuging for five cycles. Finally, the silver flakes were dried in vacuum before SEM observations and TGA tests. The morphologies of untreated silver flakes and silver flakes treated with PEG were observed by field-emission SEM (LEO 1530). The weight loss of untreated and PEG-treated silver flakes during heating was studied by TGA (TA Instruments, Q50) at a heating rate of 5 °C min^{-1}.

The storage modulus of the PU-ECA film was measured using a DMA (TA Instruments, 2980) in tension mode. The sample was heated from 0 °C to 100 °C at 5 °C min^{-1} with a constant frequency of 10 Hz.

The lap shear test was performed according to ASTM D1002. To eliminate the effects of the thickness of adhesives on the adhesion strength,[40] 0.5 wt% of glass beads with uniform diameter of 75 μm were added to the adhesives to serve as "spacers". When applying a compression force during the curing of the adhesives, the thickness of all the samples was kept around 75 μm.

A DC power supply (Hewlett–Packard 6553A) was used to power the LED chips (Lite-On, 160-1458-1-ND).

The simulation of the antenna performance was conducted using high-frequency structural simulator (HFSS) (Ansys Inc.). The S_{11} parameter was measured using a VNA (Agilent, 85052D).

Supporting Information

Supporting Information is available from the Wiley Online Library or from the author.

Acknowledgements

This work was partly supported by the Ministry of Knowledge Economy, Republic of Korea.

Received: August 9, 2012
Revised: September 12, 2012
Published online: October 19, 2012

[1] S.-I. Park, Y. Xiong, R.-H. Kim, P. Elvikis, M. Meitl, D.-H. Kim, J. Wu, J. Yoon, C.-J. Yu, Z. Liu, Y. Huang, K.-C. Hwang, P. Ferreira, X. Li, K. Choquette, J. A. Rogers, *Science* **2009**, *325*, 977.
[2] C. Yang, W. Lin, Z. Li, R. Zhang, H. Wen, B. Gao, G. Chen, P. Gao, M. M. F. Yuen, C. P. Wong, *Adv. Funct. Mater.* **2011**, *21*, 4582.
[3] A. Russo, B. Y. Ahn, J. J. Adams, E. B. Duoss, J. T. Bernhard, J. A. Lewis, *Adv. Mater.* **2011**, *23*, 3426.
[4] T. Sekitani, T. Yokota, U. Zschieschang, H. Klauk, S. Bauer, K. Takeuchi, M. Takamiya, T. Sakurai, T. Someya, *Science* **2009**, *326*, 1516.
[5] L. Han, K. Song, P. Mandlik, S. Wagner, *Appl. Phys. Lett.* **2010**, 96.
[6] K. Takei, T. Takahashi, J. C. Ho, H. Ko, A. G. Gillies, P. W. Leu, R. S. Fearing, A. Javey, *Nat. Mater.* **2010**, *9*, 821.
[7] Z. Fan, H. Razavi, J.-W. Do, A. Moriwaki, O. Ergen, Y.-L. Chueh, P. W. Leu, J. C. Ho, T. Takahashi, L. A. Reichertz, S. Neale, K. Yu, M. Wu, J. W. Ager, A. Javey, *Nat. Mater.* **2009**, *8*, 648.
[8] J. Yoon, A. J. Baca, S.-I. Park, P. Elvikis, J. B. Geddes, L. Li, R. H. Kim, J. Xiao, S. Wang, T.-H. Kim, M. J. Motala, B. Y. Ahn, E. B. Duoss, J. A. Lewis, R. G. Nuzzo, P. M. Ferreira, Y. Huang, A. Rockett, J. A. Rogers, *Nat. Mater.* **2008**, *7*, 907.
[9] L. Hu, H. Wu, F. La Mantia, Y. Yang, Y. Cui, *ACS Nano* **2010**, *4*, 5843.
[10] L. Hu, J. W. Choi, Y. Yang, S. Jeong, F. La Mantia, L.-F. Cui, Y. Cui, *Proc. Natl. Acad. Sci. USA* **2009**, *106*, 21490.
[11] M. C. LeMieux, Z. N. Bao, *Nat. Nanotechnol.* **2008**, *3*, 585.
[12] J. A. Rogers, T. Someya, Y. Huang, *Science* **2010**, *327*, 1603.
[13] S. P. Lacour, J. Jones, S. Wagner, T. Li, Z. Suo, *Proc. IEEE* **2005**, *93*, 1459.
[14] B. D. Gates, *Science* **2009**, *323*, 1566.
[15] X. Hu, P. Krull, B. de Graff, K. Dowling, J. A. Rogers, W. J. Arora, *Adv. Mater.* **2011**, *23*, 2933.
[16] D.-H. Kim, J. A. Rogers, *Adv. Mater.* **2008**, *20*, 4887.
[17] J. Lee, J. Wu, M. Shi, J. Yoon, S.-I. Park, M. Li, Z. Liu, Y. Huang, J. A. Rogers, *Adv. Mater.* **2011**, *23*, 986.
[18] Y. Sun, W. M. Choi, H. Jiang, Y. Y. Huang, J. A. Rogers, *Nat. Nanotechnol.* **2006**, *1*, 201.
[19] T. Li, Z. Huang, Z. Suo, S. P. Lacour, S. Wagner, *Appl. Phys. Lett.* **2004**, *85*, 3435.
[20] S. P. Lacour, S. Wagner, Z. Huang, Z. Suo, *Appl. Phys. Lett.* **2003**, *82*, 2404.
[21] B. Y. Ahn, E. B. Duoss, M. J. Motala, X. Y. Guo, S. I. Park, Y. J. Xiong, J. Yoon, R. G. Nuzzo, J. A. Rogers, J. A. Lewis, *Science* **2009**, *323*, 1590.
[22] H. M. Lee, S. Y. Choi, K. T. Kim, J. Y. Yun, D. S. Jung, S. B. Park, J. Park, *Adv. Mater.* **2011**, *23*, 5524.
[23] A. Garcia, J. Polesel-Maris, P. Viel, S. Palacin, T. Berthelot, *Adv. Funct. Mater.* **2011**, *21*, 2096.
[24] H. Cong, T. Pan, *Adv. Funct. Mater.* **2008**, *18*, 1912.
[25] M. A. Lutz, R. L. Cole, in *Proc. 39th Electronic Components and Technology Conf.*, IEEE **1989**, 83.
[26] H. Jiang, K.-S. Moon, Y. Li, C. P. Wong, *Chem. Mater.* **2006**, *18*, 2969.
[27] R. Zhang, W. Lin, K.-S. Moon, C. P. Wong, *ACS Appl. Mater. Interfaces* **2010**, *2*, 2637.
[28] K.-Y. Chun, Y. Oh, J. Rho, J.-H. Ahn, Y.-J. Kim, H. R. Choi, S. Baik, *Nat. Nanotechnol.* **2010**, *5*, 853.
[29] R. Ma, S. Kwon, Q. Zheng, H. Y. Kwon, J. I. Kim, H. R. Choi, S. Baik, *Adv. Mater.* **2012**, *24*, 3344.
[30] J. C. Agar, K. J. Lin, R. Zhang, J. Durden, K.-S. Moon, C. P. Wong, in *Proc. 60th Electronic Components and Technology Conf. (ECTC)*, IEEE **2010**, 1226.
[31] R. Zhang, K.-S. Moon, W. Lin, J. C. Agar, C.-P. Wong, *Compos. Sci. Technol.* **2011**, *71*, 528.
[32] D. Lu, C. P. Wong, *Int. J. Adhes. Adhes.* **2000**, *20*, 189.
[33] D. Lu, Q. K. Tong, C. P. Wong, *IEEE Trans. Compon. Packag. Technol.* **1999**, *22*, 223.
[34] D. Lu, C. Wong, *J. Therm. Anal. Calorim.* **2000**, *59*, 729.
[35] D. Lu, C. Wong, *J. Therm. Anal. Calorim.* **2000**, *61*, 3.
[36] D. Lu, C. P. Wong, *IEEE Trans. Compon. Packag. Technol.* **2000**, *23*, 440.
[37] M. Popa, T. Pradell, D. Crespo, J. M. Calderon-Moreno, *Colloids Surf., A.* **2007**, *303*, 184.
[38] L. B. Luo, S. H. Yu, H. S. Qian, T. Zhou, *J. Am. Chem. Soc.*, **2005**, *127*, 2822.
[39] S. I. Park, J. H. Ahn, X. Feng, S. D. Wang, Y. G. Huang, J. A. Rogers, *Adv. Funct. Mater.* **2008**, *18*, 2673.
[40] R. Kahraman, M. Sunar, B. Yilbas, *J. Mater. Process. Technol.* **2008**, *205*, 183.